ORIGINAL

Heat transfer from a flat surface to an inclined impinging jet

M. Attalla · M. Salem

Abstract An experimental study was carried out to investigate the effect of the inclination jet on convection heat transfer to horizontal flat plate. Local heat transfer determined as a function is of three parameters including inclination angle of the air jet relative to the plate in range of $90° \leq \theta \leq 45°$, jet-to-plate spacing in range of $2 \leq L/D \leq 8$ and Reynolds number in range of $1{,}500 \leq Re \leq 30{,}000$. The results show that the maximum heat transfer point moves towards the uphill side of the plate and the maximum heat transfer decreases as the inclination angle decreases. The correlations were conducted to predict maximum and local Nusselt number as a function of Re, θ, L/D, and x/D for a specific three regions.

List of symbols

A	Surface area (m^2)
D	Inner diameter (m)
h	Convection heat transfer coefficient ($W/m^2 K$)
I	Current (A)
k_{air}	Thermal conductivity of air (W/m K)
L	Height of nozzle above the surface (m)
Nu	Nusselt number (–)
Q_{conv}	Convection heat flux (W/m^2)
Q_{ele}	Electrical power per unit area (W/m^2)
Q_{loss}	Loss heat flux (W/m^2)
Q_{nat}	Natural convection heat flux (W/m^2)
Q_{rad}	Radiation heat flux (W/m^2)
Re	Reynolds number (–)
S	Displacement of maximum heat transfer from the geometrical impingement point (m)
T_∞	Ambient temperature (°C)
T_j	Jet exit temperature (°C)
T_s	Surface temperature (°C)
V	Voltage (V)
x	Distance along the plate in horizontal direction (m)

Greek symbols

ε	Emissivity (–)
θ	Jet inclination angle (°)
σ	Stefan–Boltzmann constant 5.65×10^{-8} ($W/m^2 K^4$)

M. Attalla (✉)
Mechanical Power and Energy Department, Faculty of
Engineering, South Valley University, Qena, Egypt
e-mail: moha_attalla@yahoo.com

M. Salem
Mechanical Department, Faculty of Industrial Education,
Sohag University, Sohag, Egypt
e-mail: mahmoudsalem.ahmed@yahoo.com

1 Introduction

Inclined impinging jet has many applications in heat transfer due to its ability to produce high localized and average area of heat transfer coefficients. For example, the inclined impinging air was jet used in cooling of a grind process [1], where it needed maximum cooling capacity. Impinging jets have also many engineering appellations such as gas turbine blades cooling and the thermal management of electronics. There is also an interest in the application on fan-powered vertical take-off and landing vehicles where the flow field can be simulated by an obliquely impinging circular air jet flow [2]. The complex nature of a turbulent impinging jet flow, a jet issuing out of a pipe or nozzle and then impinging on a target surface with change of flow direction upon impingement, makes it difficult to rely on analytical solution to predict the heat transfer process between the jet and the target plate [2].

The main variables of jet impingement heat transfer are the angle of impingement surface jet, Reynolds number and the height of the nozzle above the impingement surface [3]. Comprehensive reviews on impinging jet heat transfer are available by Janbunathan et al. [4] and Martin [5]. The majority of studies have focused on jet impingement on flat surface with transfer characteristics from a single or multiple vertical impinging jets. For a vertical circular jet impinging on a flat plate, it was concluded from early experimental results that for stagnation region, the maximum heat transfer happens at a jet-to-plate distance of about six times the jet diameter [6].

Impinging jets with an inclined angle were presented in many applications. The imposed complexity attributed to the inclined angles in the fluid flow and heat transfer could add to the problem of non-uniform heating or cooling of impinging jets in industrial process [2]. It is, therefore, important to understand the effect of obliqueness of an impinging jet to the heat transfer characteristics.

A few studies that have investigated the effect of jet inclined angles on flow field and heat transfer. Yan and Saniei [2] investigated the heat transfer from a flat plate to an air jet impinging obliquely from a circular nozzle using the preheated wall transient liquid crystal technique. Their results showed that the point of the maximum heat transfer shifts away from the geometrical impingement point towards the uphill side of the plate. Donovan and Murray [3] reported the fluid flow and heat transfer distribution to an obliquely impinging air jet. They proved that the velocity stagnation point (zero velocity) shifted to uphill direction with decreasing of inclined jet angle. In addition, the surface heat transfer decreases sharply towards the uphill direction and more gradually in the downhill direction. Beltos [7] investigated the wall pressure and shear stress in the impingement region of an oblique circular turbulent jet. The jet Reynolds number ranged from 35,000 to 10,000. The results showed that the shear stress components normal to the radial plane were small.

Sparrow and Lovell [8] used naphthalene mass-transfer technique and studied the heat transfer characteristics of an obliquely impinging circular air jet on a flat plate. Their results showed that the maximum point of heat transfer shifted from the geometrical impingement point along the axis of symmetry. Ward et al. [9] measured the heat transfer rate between a circular air jet impinging onto a uniform cross flow of air over a flat plate coated with naphthalene along with the Chilton–Colburn analogy and they obtained local heat transfer profiles. The maximum value of heat transfer rate that was found depended on the impinging jet angle and velocity ratio between the impinging jet and the cross flow.

Goldstein and Franchet [10] investigated the measured local heat transfer from an oblique nozzle to a flat plate.

The impinging jet was issued from a square edge orifice with jet-to-plate distance varied from 4 to 10. The heat flux was provided by passing an electrical flow through a thin metallic foil, while the temperature was monitored using the temperature sensitive liquid crystal technique. The results showed that the displacement of the peak heat transfer location was mainly due to the angle of inclination. A heat transfer correlation was developed for the Nusselt number as a function of jet oblique angle and jet-to-plate distance.

Some typical numerical simulations of flow field and heat transfer using k–ε turbence model were investigated by Hwang et al. [11], Hwang and Tsou [12], and Chuang and Wei [13]. In those cases, very large jet-to-plate distance and high Reynolds number were used. In addition, Garg and Jayaraj [14] used a finite-difference method to determine the temperature and velocity profiles for a laminar boundary layer generated by an inclined two-dimensional jet.

The objective of this study is to investigate the effect of jet inclination on impingement heat transfer for a single circular jet. The experiments were performed using circular nozzle with inner diameter of 9.53 mm and the exit jet Reynolds number varied from 1,500 to 30,000. Local heat transfer measurements were conducted with jet inclination angle from 90° to 45°. Correlations were developed to predict the local heat transfer and hence the magnitude of the maximum heat transfer coefficient.

2 Experimental apparatus and method

2.1 Experimental apparatus

The main parts of the experimental apparatus were a nozzle and an impingement surface shown in Fig. 1a. Air was supplied with an air compressor through a calibrated orifice flow meter. An air filter and a pressure regulator are installed upstream of the orifice flow meter to filter the air and to maintain the downstream pressure at 8 bar. The actual flow rate is controlled by needle valve before inter the digital flow rate (SITRANS FUG1010–Simens Co.). The nozzle is a stainless steel pipe of inner diameter of 9.53 mm and length to diameter ratio of 76. This length ensures a fully developed flow over the Reynolds number range investigation. The nozzle is clamped on a carriage in an arrangement that allows its height above the impingement surface and its angle of impingement to be varied.

The impinging plate (225 mm × 425 mm × 1.0 mm thick stainless steel sheet) and clamped tightly and stretched between two copper bus bars. Approximately 8 mm of the sheet on either side is sandwiched in the bus bars to ensure firm grip. Because of the sheet is thinness of sheet,

Fig. 1 a Schematic of the experimental apparatus. *1* air filter, *2* air compressor, *3* air receiver, *4* air filter, *5* pressure regulator, *6* valve, *7* data acquisition unite, *8* digital flow meter, *9* plenum chamber, *10* circular nozzle, *11* target plate, *12* data acquisition unite, *13* infrared camera, *14* adjustable stand. **b** Schematic diagram of an inclination impinging jet
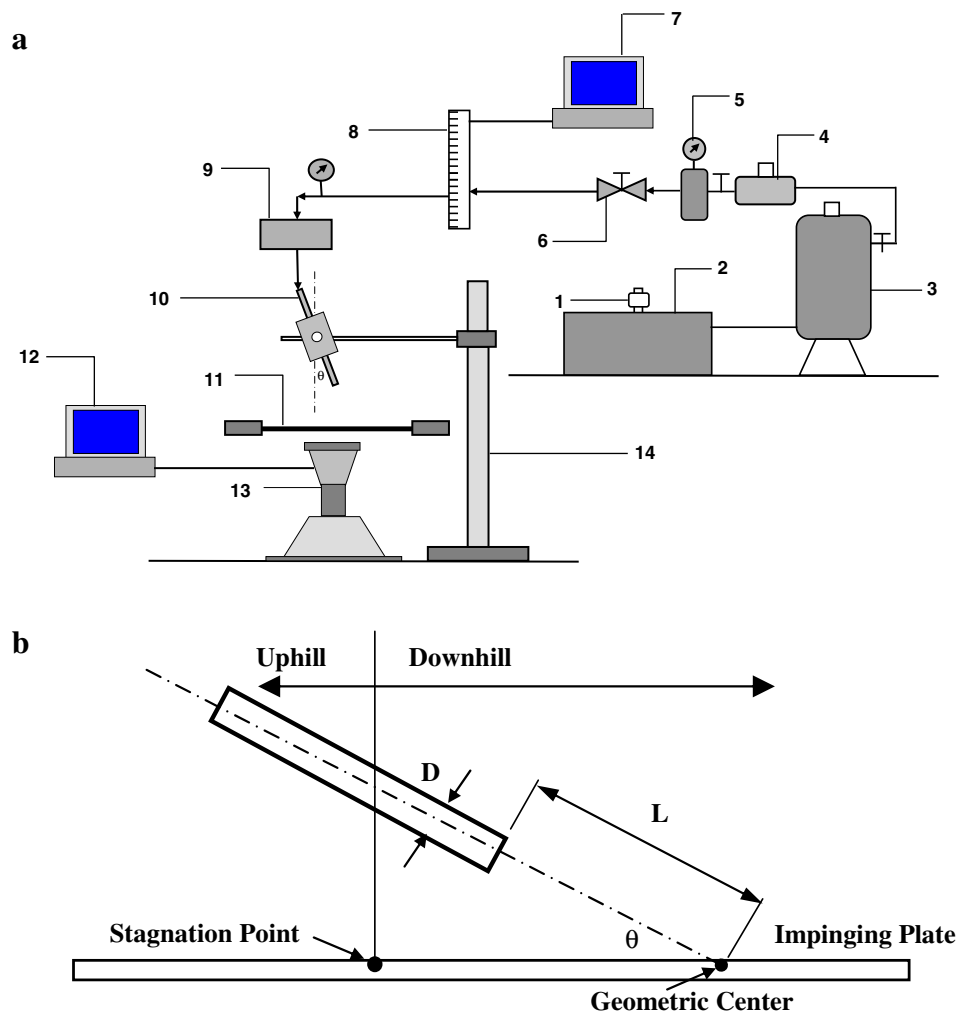

lateral conduction is negligible and surface provides constant heat flux situation as reported by Attalla and Specht [15]. Figure 1b illustrates two directions that are commonly referred to as the uphill and downhill direction of the flow.

The thermal images were obtained by IR camera (TROTEC IC120LV) which was positioned under the heated plate opposite the impinging nozzle, as in Fig. 1a. The infrared camera was used to measure local temperature from uniform heat flux surface, which provides higher spatial resolution (525 × 325 pixels) of temperature than thermocouples. TROTEC IC120VL infrared camera was used to record the local temperature distribution with resolution of 0.25 mm per pixel. One dimensional energy balance across the heated plate shows negligible temperature difference across it, therefore the local temperature difference on the bottom surface is considered the same as that on the top side. The bottom side of heated plate is painted using a thin coat of ACRYLIC AG: 525 paint which provides high emissivity.

The impinging plate was heated using AC power source through a voltage stabilizer. The voltage and current are measured by LUCAS-NÜLLE-LM2332 digital meters whose ranges and the accuracies are of 400 mV–400 V ±0.5 % and 20 mA–400 A ±0.8 % respectively. The air jet temperature is measured using a hot-wire thermo-anemometer (CFM-thermo-Anemometer—Model 407119A) positioned at the outlet of the nozzle.

Thermal infrared camera reads the temperature of the plate depending on the emissivity value of the plate surfac. Therefore, it is necessary to calibrate the emissivity of the surface [16]. This was done by constructing a 15 cm size cubical tank from the same material as that of the target plate. This tank is painted with ACRYLIC AG: 525 black paint to achieve uniform emissivity all over the surface. The tank is insulated from the five sides and one is opened to the atmosphere. Tank is filled with water and is heated with 400 W heaters. A small motor driven stirrer is immersed in the water to maintain uniform temperature of the water bath. Two calibrated thermocouples are mounted on the exposed

Fig. 2 Schematic diagram of surface emissivity measured. *1* DC motor, *2* stirrer, *3* tank, *4* insulation, *5* heater, *6* thermocouple, *7* data acquisition unite, *8* infrared camera
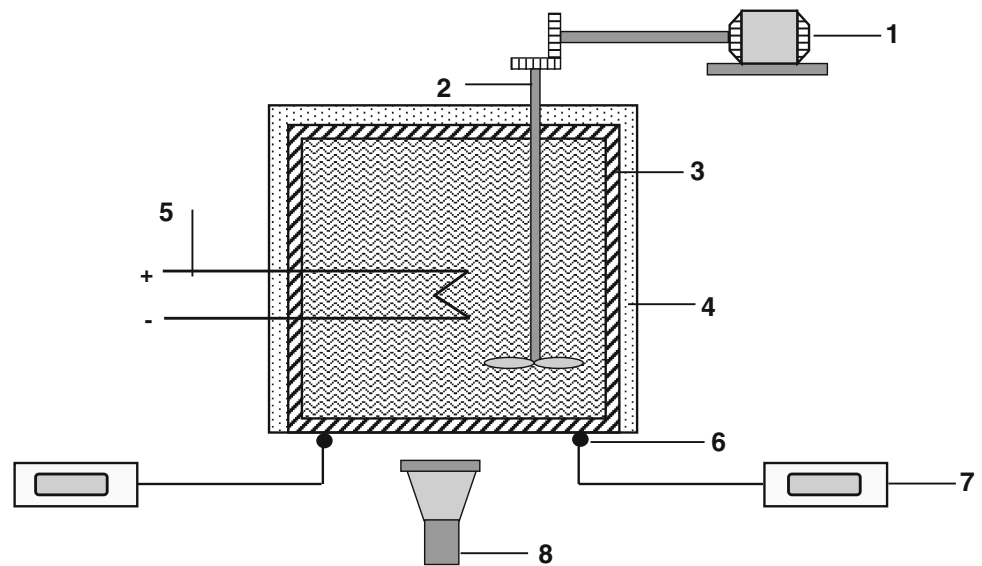
surface of the tank at two different locations as shown in Fig. 2. Initially, water in the tank is heated to temperature of about 75 °C, then the heater is switched off and the temperature of the surface is allowed to decrease. The time constant of temperature drop is about 2 min per 0.5 °C. This time is sufficient to obtain thermal image of the surface from the infrared camera and thermocouples reading. The emissivity input to the image setting is then adjusted until the temperature is read the infrared camera reads the same as that by thermocouples. This procedure is repeated for different temperatures of the exposed surface until it reached 30 °C. The average emissivity is found to be 0.95.

2.2 Procedure and data reduction

The temperature distribution on the impinging plate is obtained by averaging three infrared thermal images for each inclined angle. The Nusselt number for the smooth surface is estimated using the following equation:

$$Nu = \frac{hD}{k_{air}} \qquad (1)$$

where, h is heat transfer coefficient (W/m^2 K), and calculated by the following equation

$$h = \frac{Q_{conv}}{T_s - T_j} \qquad (2)$$

where T_S and T_j are surface and jet temperatures respectively.

The heat transfer rate between impinging jet and target plate, Q_{CONV}, is estimated as follows [16]:

$$Q_{conv} = Q_{ele} - Q_{loss} \qquad (3)$$

$$Q_{loss} = Q_{rad} + Q_{nat} \qquad (4)$$

$$Q_{ele} = \frac{VI}{A} \qquad (5)$$

where

$$Q_{rad} = \varepsilon\sigma\left(T_s^4 - T_\infty^4\right) \qquad (6)$$

2.3 Uncertainty of experimental

The uncertainty in Nusselt number was influenced primarily by the determination of heat flux and wall temperature. The surface heat flux was affected by the variation of the constantan metal sheet thickness that was claimed in the suppliers' specification to be less than ±5 % of the normal value. The Nusselt number uncertainties were carried out using the method suggested by Moffat [17], and ranged from 4.5 to 9.75 %. The uncertainty in Reynolds number was affected by the measurement of the flow rates and the nozzle exit area. The airflow rate was measured by calibrate flow meter ±5.5 %, and not excess ±8.3 %. Another source of the uncertainty in wall temperature was disturbed with lateral heat conduction along the constantan metal sheet by the sharp radial variation of the Nusselt number around the stagnation zone [18]. The thermocouples were used to measure the surface emissivity calibrated to an uncertainty of ±0.35 K before experiments.

3 Results and discussion

3.1 Displacement of stagnation point heat transfer

The stagnation/maximum heat transfer point was an important phenomena observed with oblique jet impingement. The displacement was measured in the present study with air jet
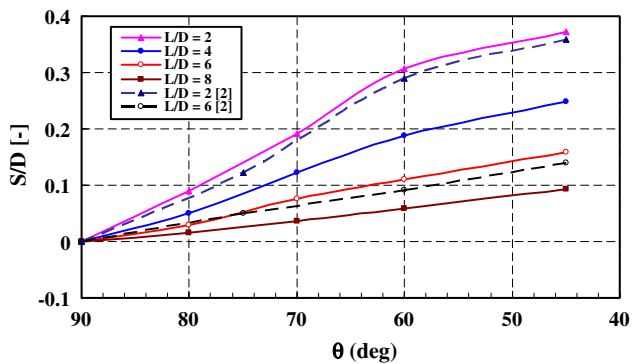
Fig. 3 Displacement of point of maximum heat transfer, Re = 23,000

Fig. 4 Effect of Reynolds number on the displacement of maximum heat transfer

issuing from a jet tube of 9.53 mm inner diameter. The shift of maximum heat transfer from the geometrical impingement point was directed toward the compression side (uphill direction) on the principle axes. The results are shown in Fig. 3 for Reynolds number 23,000, and different values of L/D. The figure shows that the displacement decreases monotonically with the increase of jet inclination angles. It is also noted that the effect of inclination angles on the displacement of maximum heat transfer is found to be sensitive to the jet-to-plate distance L/D. As the jet moves away from the plate L/D > 6, the free jet flow has a uniform momentum before impinging on the surface. The asymmetric momentum transport process associated with a skewed velocity field was responsible for the displacement of maxima or minima of related quantities [3]. The effect of inclination angle became minimum with large L/D. This is consistent with the surface stagnation pressure measurement of Beltos [7], where value of very large jet-to-plate distance (L/D = 15–47) was used. Beltos [7] speculated that the position of maximum pressure might not be the same point as the stagnation point (zero velocity), and neither might coincide with the point of maximum heat transfer point. The results obtained by Xiaojoun and Nader [2] for circular air jet are shown in Fig. 3 for comparison with the present results of Reynolds number 23,000 of L/D = 2, 4. It is found from the comparison that the maximum values of displacement measured from the two studies are quite close to the current results.

Figure 4 shows the shift of point of maximum heat transfer for a fixed jet-to-plate distance L/D = 4 for three Reynolds numbers 1,500, 15,000, and 23,000. The lower Reynolds number, 1,500, is the lower value the displacement of maximum heat transfer is than the other Reynolds numbers 15,000 and 23,000.

3.2 Local heat transfer coefficient profiles

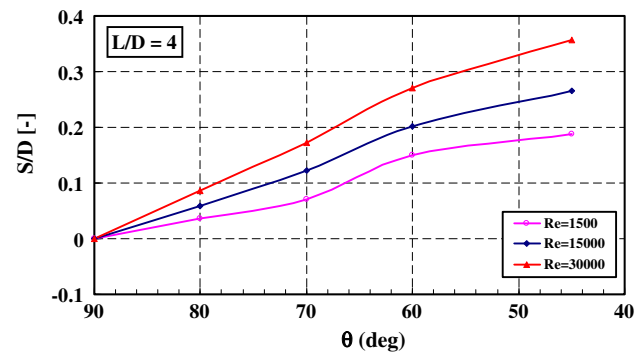The main target of the current study is to measure profiles of local Nusselt number at representative values of Reynolds number and jet inclination angle. The local heat transfer was measured and plotted as a function of radial position along principal horizontal (x) axis, with origin situated at the point of maximum heat transfer. The results were also presented for various jet angles (90°, 80°, 70°, 60°, 45°) in Figs. 5 and 6.

3.2.1 Effect of inclination angle

Figures 5 and 6 show the detailed local heat transfer coefficient distribution for five different inclination angles, θ = 90°, 80°, 70°, 60°, 45° for jet-to-plate distance of 2 and 6. The local heat transfer distributions for a jet impinging at a range of inculcation angles and maximum Reynolds number Re = 30,000 are shown in Fig. 5a, b for jet-to-plate spacing of L/D = 2 and L/D = 6, respectively. The first spacing distance of where the impingement plate was within the potential core of the jet, while the second spacing to a location just beyond the core of the jet. In the case of angle θ = 90°, there was normal jet impingement on plate and the local heat transfer was symmetrical around the central point of the test plate. The maximum heat transfer point shifts towards the uphill side of the plate from the geometrical point as the jet angle decreases. The results were close to the results from Donovan and Murray [3] who measured the flow field and heat transfer from inclination jet impinging into flat plate. They proved that the velocity stagnation point shifted to uphill with decreasing the incline jet angle. In addition, these figures show that the shift of maximum heat transfer was clearly observed for small value of L/D = 2 and it increased with decreasing the jet inclination angle. With the large spacing distance of 6, the amount of the increase in the maximum heat transfer point decays gradually. In the heat transfer measurement, the location of the displacement of the maximum heat transfer appeared at 1.4D from the geometrical center of the plane.

It was well documented by Goldstein et al. [19], Baughn and Shimizu [20], Rubel [21] and Beitelmal et al. [22] for
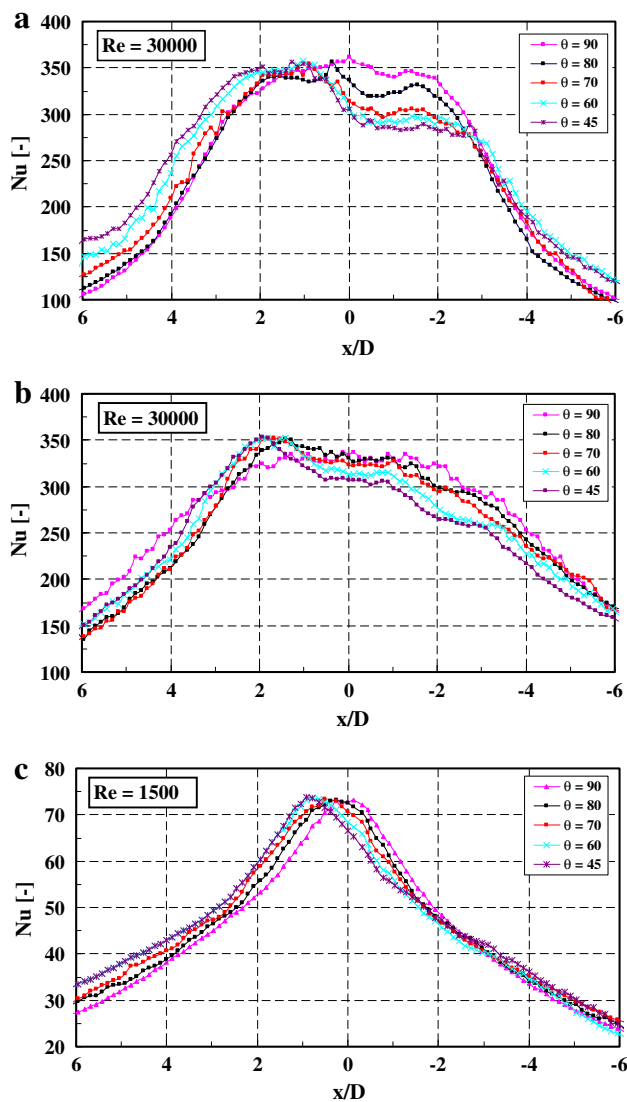
Fig. 5 a Variation local Nusselt number with different values of θ at L/D = 2. **b** Variation local Nusselt number with different values of θ at L/D = 6. **c** Variation local Nusselt number with different values of θ at L/D = 6

Fig. 6 a Variation local Nusselt number with different values of L/D at θ = 60°. **b** Variation local Nusselt number with different values of L/D at θ = 45°

3.2.2 Effect of jet-to-plate distance

The effect of jet-to-plate distance on local heat transfer can be shown in Fig. 6a, b. Figure 6a, b show the potted of local Nusselt number versus x/D for different values of L/D (2 ≤ L/D ≤ 8), at constant value of Reynolds number (Re = 23,000) for two incline angles (θ = 60° and 45°). The shift of point of maximum heat transfer was clearly observed. The heat transfer rate distribution on the compression side showed monotonic decreasing beyond the maximum point. As the jet-to-plate distances increased, the drop of heat transfer on the downhill direction became less rapid. The figures also show that for radial distance beyond scattering of heat transfer became less pronounced with the increase of L/D. This indicates that at the larger distances (beyond the jet potential core), the jet is so well mixed and spread. This was due to that the heat transfer distribution on the plate was less sensitive to the jet-to-pate distance.

3.3 Local Nusselt number correlation

In the current study, the local Nusselt number was correlated as a function of the four parameters involved L/D, x/D, θ and jet exit Reynolds number. Correlations were developed for three regions: the stagnation region

low nozzle to impingement plate spacing, secondary peaks in the Nusselt number distribution occur at a radial location of approximately 1–3 diameter from the geometric center for a normally impinging jet (θ = 90°). Figure 5a, b shows that these peaks in Nusselt number distribution occur for inculcation jet impingement also for high Reynolds number Re = 30,000, but this feature is not present in the data shown in Fig. 5c where L/D = 6 and Re = 1,500. It can also be observed from the results presented in Fig. 5a–c that secondary peaks may not occur in the uphill direction. For example, there is no secondary peak in uphill direction when jet inclination into plate of θ = 60°, but a broad secondary peak does occur in the downhill direction.
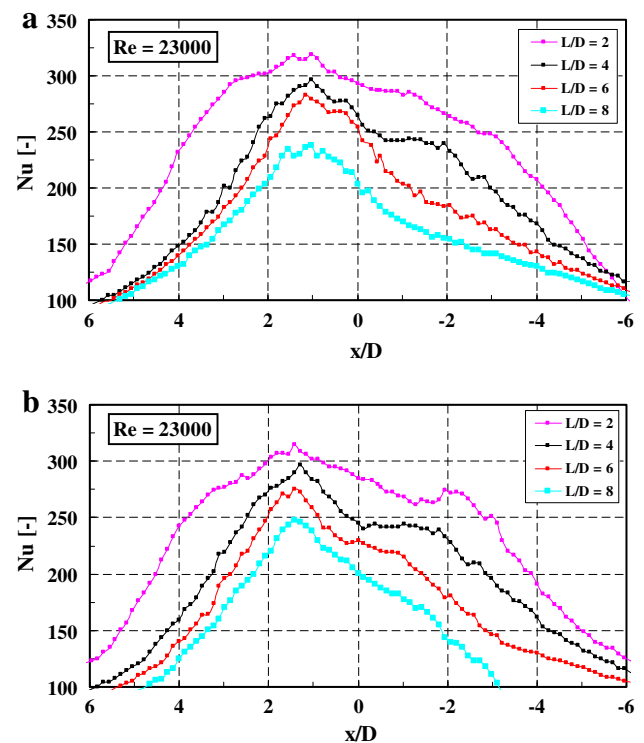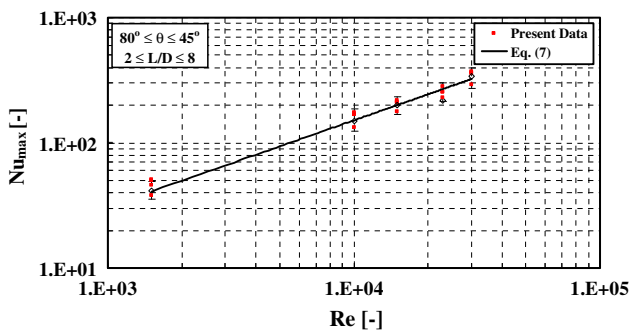
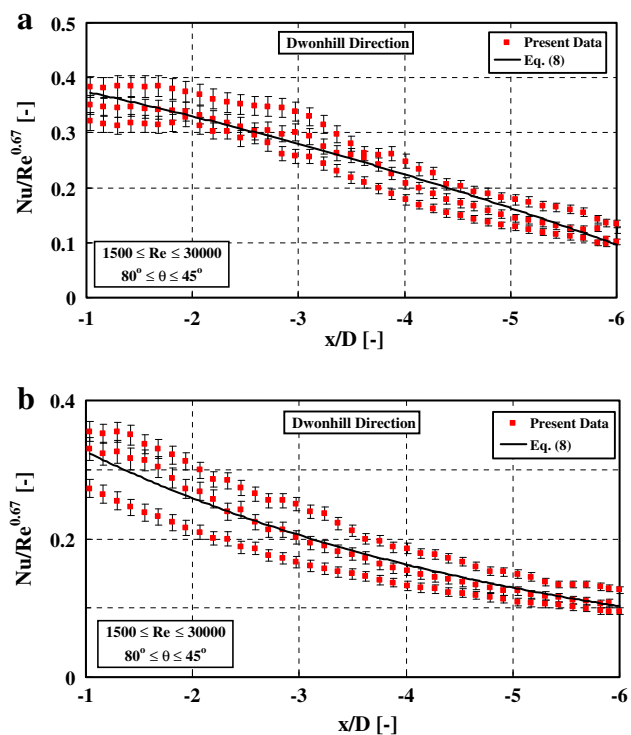**Fig. 7** The maximum Nusselt number correlation for the present data

Fig. 8 a The Nusselt number correlation for the present data along the major axis at L/D = 2. **b** The Nusselt number correlation for the present data along the major axis at L/D = 4

(maximum Nusselt number), major axis (downhill region) and minor axis (uphill region) [22].

The maximum values of the Nusselt number (stagnation region) were obtained from the experimental data, and were used to develop the following correlation:

$$Nu_{max} = 0.29 \text{Re}^{0.69} \text{Pr}^{0.33} (\sin \theta)^{0.52}$$
$$\times (L/D)^{-0.045} \begin{cases} 1{,}500 \leq \text{Re} \leq 30{,}000 \\ 2 \leq L/D \leq 8 \\ 80^\circ \leq \theta \leq 45^\circ \end{cases} \tag{7}$$

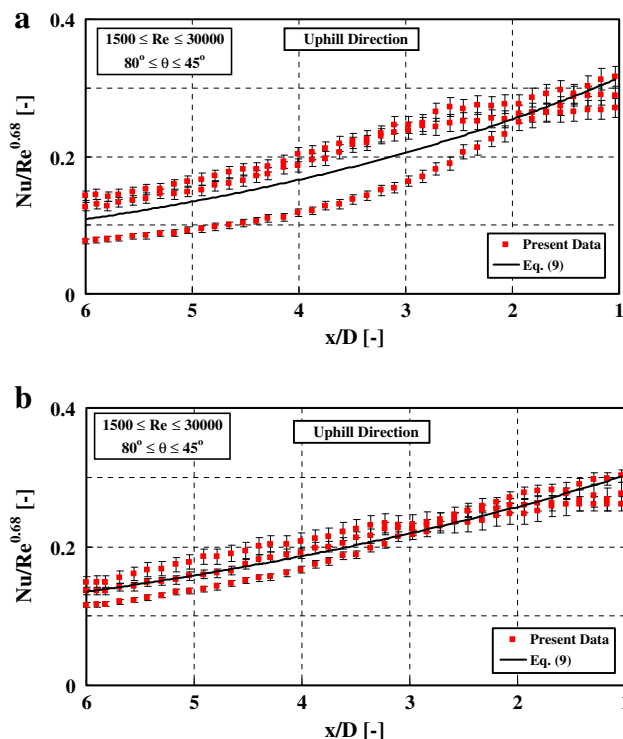The above correlation fits the present data to within 3.5 % as shown in Fig. 7.

Fig. 9 a The Nusselt number correlation for the present data along the minor axis at L/D = 2. **b** The Nusselt number correlation for the present data along the minor axis at L/D = 4

The local Nusselt number data for the downhill side were correlated by the following empirical equation:

$$Nu = 0.345 \text{Re}^{0.67} \text{Pr}^{0.33} (1.29 \sin \theta)^{0.954}$$
$$\times (L/D)^{-0.019} (\text{x}/D)^{-0.03} \begin{cases} 1500 \leq \text{Re} \leq 30000 \\ 2 \leq L/D \leq 6 \\ 80^\circ \leq \theta \leq 45^\circ \\ 1.25 \leq \times /D \leq 6 \end{cases} \tag{8}$$

The above equation fits the present data with maximum deviation of 6.32 % as shown in Fig. 8a, b for differences values of L/D.

For uphill wall jet, it was possible to correlate the local Nusselt number distribution with a reasonable maximum deviation. The local Nusselt number results were correlated as the following equation;

$$Nu = 0.297 \text{Re}^{0.68} \text{Pr}^{0.33} (1 + 0.37 \sin \theta)^{0.97}$$
$$\times (L/D)^{-0.02} (\text{x}/D)^{-0.027} \begin{cases} 1{,}500 \leq \text{Re} \leq 30{,}000 \\ 2 \leq L/D \leq 6 \\ 80^\circ \leq \theta \leq 45^\circ \\ 1.20 \leq \text{x}/D \leq 5.5 \end{cases} \tag{9}$$

The above equation fits the present data with maximum deviation of 7.45 % as shown in Fig. 9a, b for differences values of L/D.

4 Conclusion

The local heat transfer characteristics of an impinging circular jet on a preheated flat plate have been experimentally investigated. The effect of the inclination angle of the plate (θ) and the spacing distance between the nozzle exit and plate (L/D) on the local heat transfer were of primary interest in the range of the Reynolds number of 1,500–30,000. The parameter ranges were $\theta = 90°$, $80°$, $70°$, $60°$, and $45°$ and L/D = 2, 4, 6, and 8. The temperature distributions over the flat plate were measured using infrared camera.

The results showed that the maximum heat transfer point moved towards the uphill side of the plate. This was due to the change in the magnitude and direction of the velocity of the air jet. The displacement depended on the angle of inclination and the vertical distance between exit nozzle and plate. At the inclination angle of 45°, the heat transfer on the downhill side of the plate was higher than that of the uphill side.

The value of maximum Nusselt number steadily increased at lower jet-to-plate spacing as the inclination decreases. As small jet-to-plate distance studied, the heat transfer distribution on the compression side (uphill) of the plate showed a monotonic rapid drop beyond the point of maximum, while the heat transfer distribution on the other (downhill) side exhibited a same pattern as that of a vertical jet-second maxima. The location of the second maximum moved away from the center as the angular direction θ decreased. This was due to the fact that vortices in downhill direction had time and space to develop and pass as large scale, while in the uphill the vortices have not completed a merging process and pass as small scale. Finally, the local Nusselt number distributions were correlated as a function of exit Reynolds number, inclination angle and jet-to-plate for three regions of the target surface: maximum region, uphill region, and downhill region.

References

1. O'Donovan TS, Murray DB, Torrance AA (2006) Jet heat transfer in the vicinity of a rotating grinding wheel. Proc Instit Mech Eng Part C J Mech Eng Sci 220:836–845
2. Yan X, Saniei N (1979) Heat transfer from an obliquely impinging circular air jet to a flat plate. Int J Heat Fluid Flow 18:591–599
3. O'Donovan TS, Murray DB (2008) Fluctuating fluid flow and heat transfer of an obliquely impinging air jet. Int J Heat Mass Transf 51:6169–6179
4. Janbunathan K, Lai E, Moss MA, Buton BL (1992) A review of heat transfer data for single circular jet impingement. Int J Heat Fluid Flow 13:106–115
5. Martin H (1977) Heat and mass transfer between impinging gas jets and solid surface. Adv Heat Mass Transf 13:1–60
6. Gardon R, Akfirat JC (1965) The role of turbulent in determining the heat transfer characteristics of impinging jets. Int J Heat Mass Transf 8:597–605
7. Beltos S (1976) Oblique impinging of circular turbulent jets. J Hydraul Res 14:17–36
8. Sparrow EM, Lovell BJ (1980) Heat transfer characteristics of an oblique circular jet, ASME. J Heat Transf 102:202–209
9. Ward J, Oladiran MT, Hammond GP (1991) Effect of nozzle inclination on jet impingement heat transfer in a confined cross flow. In: ASME 91-HTD, vol 181, pp 25–31
10. Goldisten RJ, Franchett ME (1988) Heat transfer from a flat plate to an oblique impinging jet. J Heat Transf 110:84–90
11. Hwang JC, Tsou FK, Cho WC (1982) Kappa-Epsilon computations of flow and heat transfer in plane oblique impinging jet. In: Computer methods experience measured, proceeding of international conference, Washington, DC, pp 271–282
12. Hwang JC, Tsou FK (1983) Numerical solutions for flow and heat transfer for plane turbulent oblique impinging jet. In: Numerical properties and methodologies in heat transfer (A84-40651 19–34). Hemisphere Publishing Corp., Washington, DC, pp 403–417
13. Chuang SH, Wei CY (1991) Computational for a jet impinging obliquely on a flat surface. Int Numer Method Fluids 12:637–653
14. Garg VK, Jayaraj S (1988) Boundary layer analysis for two dimensional slot jet impingement on inclined plates. J. Heat Transf 110:577–582
15. Attalla M, Specht E (2009) Heat transfer characteristics from in-line arrays of free impinging jets. J Heat Mass Transf 45:537–543
16. Vadiraj K, Prabhu SV (2008) Experimental study and theoretical analysis of local heat transfer distribution between smooth flat surface and impinging air jet from a circular straight pipe nozzle. Int J Heat Mass Transf 51:4480–4495
17. Moffat RJ (1988) Describing the uncertainties in experimental results. J Fluid Sci 1:3–17
18. Ma CF, Zheng Q, Sun H, Wu K, Horii K (1998) Local convention heat transfer from a vertical flat surface to oblique submerged impinging jets of large Prandtl number liquid. Exp Thermal Fluid Sci 17:238–247
19. Goldisten RJ, Behbahain I, Heppelmann K (1986) Stream-wise distribution of the recovery factor and the local heat transfer coefficient to an impinging circular air jet. Int J Heat Mass Transf 29:1227–1235
20. Baughn JW, Shimizu SS (1989) Heat transfer measurements from a surface with uniform heat flux and an impinging jet. ASME J Heat Transf 111:1096–1098
21. Rubel A (1982) Oblique impingement of a round jet on plane surface. AIAA J 20:1756–1758
22. Beitelmal AH, Michel AS, Chandrakant DP (2000) The effect of inclination on the heat transfer between a flat surface and an impinging two-dimensional air jet. Int J Heat Fluid Flow 21:156–163